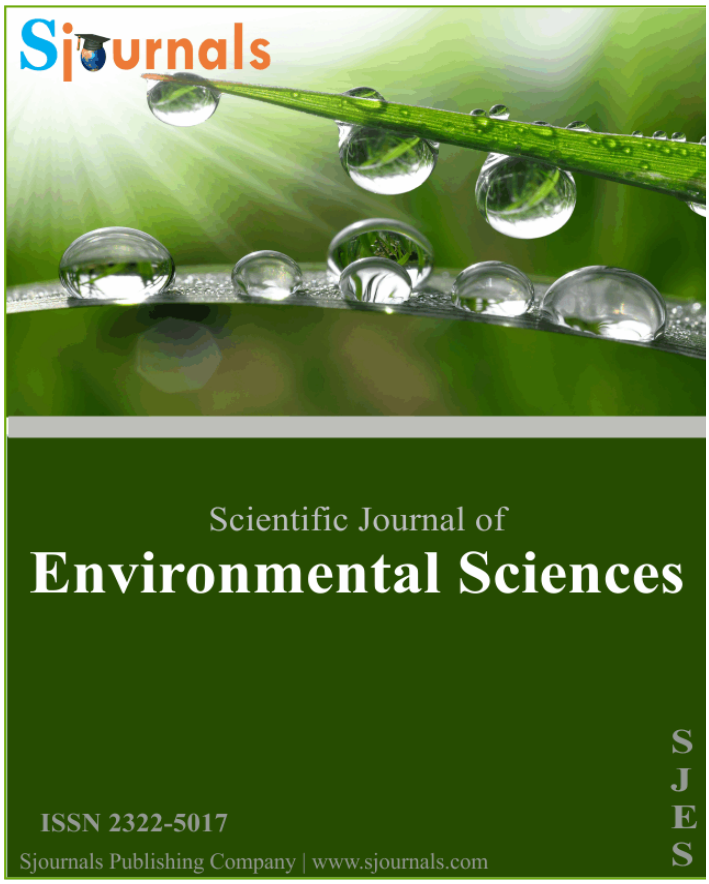

Scientific Journals

Scientific Journal of Environmental Sciences (2016) 5(11) 269-278
ISSN 2322-5017
doi: 10.14196/sjes.v5i11.2292

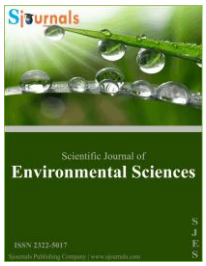

Contents lists available at Sjournals

Scientific Journal of **Environmental Sciences**

Journal homepage: www.Sjournals.com

**Original article**

# Numerical investigation on packing density and inlet configurations of hollow fibres and their effects on flow pattern within ultrafiltration modules

**Keng Boon Lim[a], Peng Cheng Wang[b,*], Hui An[b]**

[a]*Professional Officers' Division, Singapore Institute of Technology, Singapore.*
[b]*Engineering, Singapore Institute of Technology, Singapore.*

*Corresponding author; Engineering, Singapore Institute of Technology, Singapore.

ARTICLE INFO

*Article history,*
Received 17 October 2016
Accepted 18 November 2016
Available online 22 November 2016
iThenticate screening 19 October 2016
English editing 16 November 2016
Quality control 20 November 2016

*Keywords,*
Hollow fibres
Ultrafiltration
Packing density
CFD
Numerical simulation

ABSTRACT

This study aims to investigate the changes in output permeate flowrate of ultrafiltration hollow fibres with double - end configuration. Different parameters such as packing density, feed pressure and location of feed inlet are studied using Computational Fluid Dynamics (CFD). This study adopts the numerical approach to predict how each of the factors influence the output (i.e. flowrate) of the filtration process. Preliminary studies were done to validate the numerical predictions against existing literature, showing good agreement with available data. The effect of packing density on hollow fibre with double-end configuration was then investigated. The ratio of allowable spaces between fibres, denoted by ε, was used to quantify the packing density. 2 sets of numerical model for double-end hollow fibre with ε ranging from 0.2 to 0.8 were simulated for fibre length of 1 metre and 2 metre respectively. Results showed that a higher ε value used in for the packing of hollow fibres lead to higher permeate flowrate. However, this increment stagnates even as ε is increased beyond 0.6. Other factors such as inlet positioning and fibre length, which affects feed pressure distribution were also investigated. Simulation results concluded that feed pressure distribution and output flowrate varies depending on where the inlet is situated. The proposed new inlet located along the fibre length also improves the uniformity of the feed pressure distribution along hollow fibres. This makes positioning of the inlet

crucial to the overall performance of the ultrafiltration module.



**1. Introduction**

Pressure Driven Membrane Filtration is one of the many processes involved in water treatment. This process makes use of porous membranes, typically in the form of hollow fibres, to remove micro particles such as pathogens and soluble salts from the feed (water from previous treatment process). The filtration process within a Hollow Fibre Membrane Module is simple. Incoming feed is pumped in to the module filled with thousands of hollow fibre membranes. The pressurised feed flows from the outside of the membrane and into the hollow centre of the fibres. As the feed flows to the fibre centre, particles larger than the pores on the membrane are excluded on the outside of the hollow fibre. This results in clean water on the inside of the hollow fibre, which flows towards the end of the fibre, where the clean water exits the module for the next step of treatment. The clean water that exits from the module is termed as permeate. Typical hollow fibre modules used in the industry are of cross-flow single-end configuration, where fibres within are sealed at one end. This configuration brings forth large pressure drop along within the hollow fibre centre from the dead-end to the exit, especially at higher feed pressure. In order to resolve this issue, several research studies have look into opening hollow fibres at both ends, referred to as double-end configuration.

Doshi et al. (1997) analytically predicted the increase in permeation flowrate within a hollow fibre module of single-end configuration when modified into a double-end configuration. They stated that if modifications were made, an increase of 47 percent in permeation flowrate is expected. The significant in performance is due to large reduction in pressure drop along the hollow fibre centre expected from opening both ends of the fibre. However, they also added that the magnitude of increase is also dependent on geometrical parameters such as inner radius, as they observed smaller increase in performance for fibres with larger inner diameter. The similar trend is also observed for increasing feed pressure. This suggests that the double-end configuration would be more effective for fibres with smaller inner diameters and for fibres operating at smaller feed pressure. Aimed to validate Doshi et al's study (1997), Soltanieh et al. (1983) devised an experiment to quantify the increase in performance for hollow fibre modules when modified to double-end configuration. Using the assumption that the effective fibre length of a double-end hollow fibre is equivalent to half of that of a single-end fibre, the experiment was conducted with two modules, one of original fibre length, and the other with fibres of 40 percent original length. Results show that the permeate flowrate have increased by about 39 percent when effective length is reduced to 40 percent. When tested with a range of different feed pressure, they also observe negative correlation between percentage increase in permeate flowrate, and inlet feed pressure.

Packing density within a hollow fibre module, which affects performance of single-end hollow fibres, have been studied in the past. This parameter quantifies how densely hollow fibres are packed within a module, in the form of a ratio of volume occupied by hollow fibres to total volume within module. Examples were of literatures by Günther et al. (2010) and Zhuang et al. (2015). Study by Günther et al. were focused on changes in velocity profile along the centre of hollow fibres due to differing packing density. They deduced that increasing packing density leads to the permeate profile along fibre length becoming non-uniform. In addition, these changes are more drastic when packing density goes beyond 0.6 (i.e. 60 percent of module occupied by hollow fibre), observing drastic decrease in filtration flux thereafter. Zhuang et al. instead focused on the characterising flux distribution profile of hollow fibre modules with different packing density. This was done using both analytical model and CFD simulation. They concluded that depending on packing density, one of three different flux profiles could occur. They are (i) uniform flux profile along axial length, (ii) flux profile with decreasing flux value as fibre approaches exit and (iii) flux profile with increasing flux value as fibre approaches exit. (i) occurs when packing density is in mid-range (i.e. packing density of 0.4), (ii) where fibres are very densely packed (packing density of 0.6 and 0.8) and (iii) where fibres are sparsely packed (packing density of 0.2).

Though most hollow fibre module designs adopt the single-end configuration, the potential of using double-end configuration should be looked at due to the promising results in pressure loss reduction and improvement in flowrate. It is therefore in this paper's interest to review the effects of adapting a double-end configuration to

hollow fibre membrane module in terms of the output flowrate and flux distribution. In addition, studies regarding packing density and other parameters were conducted on hollow fibres with single-end configuration. Finally, this paper will also looked into detail how various parameters such as packing density and inlet configurations will affect double-end hollow fibre the same way as single hollow fibre.

For this study, the effects of packing density, inlet pressure and locations of feed inlet on pressure profile, flux profile and outlet flowrate will be studied. The filtration process of a double-end hollow fibre will be modelled and simulated numerically. Different packing density and inlet conditions will be imposed on the model and result will be compared. The results from the numerical prediction aimto identify the changes in performance of a double-end hollow fibre, when subjected to various packing density and feed pressure. Finally, this study aims to identify and understand the effect on pressure and flux distribution when inlet locations are changed.

## 2. Methodology

### 2.1. Numerical model

The numerical models of double-end hollow fibres were modelled based on Günther et al.'s and Zhuang et al.'s model of single-end outside-in hollow fibres. Numerical models of fibres used in both studies were simplified using several assumptions presented. Bundles of hollow fibres within module are first assumed to be the same dimension and equally spaced using Happel's (1959) free surface model (Figure 1). As fibres are equally spaced, distance between each fibres are equal. This allowed the use of a single fibre to represent a bundle of fibres, regardless of fibre count.

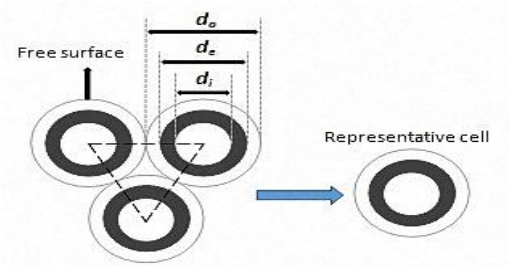


**Fig. 1.** Assumption made based on Happel's Free Surface Model shown in Günther et al. and Zhuang et al.'s work.

The second assumption assumed that the fibres have equal membrane thickness throughout. This assumption makes the representative fibre concentric, allowing the 2 dimensional axisymmetric simplification to be used. This simplifies the three dimensional model into a two dimensional model, increasing the efficiency of numerical simulations done. The numerical model was separated into three distinct zones. These regions are feed, which is the outer fluid region surrounding the membrane wall, membrane wall, the porous region where filtration takes place and permeate, where the filtered water flows towards the exit. Since this study is focused on hollow fibres with double-end configuration, the numerical model is modified to reflect the double-end configuration. Figure 2 shows a schematic diagram of the modified model.

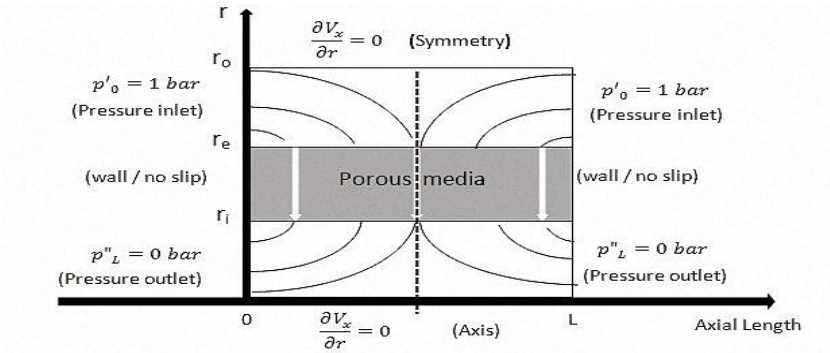


**Fig. 2.** Schematic diagram of double-end hollow fibre used in this study, with prediction of water flow pattern illustrated (Zhuang et al., 2015).

The packing density of a hollow fibre module was quantified using the ratio of allowable space between fibres, denoted by the symbol ε. This ε value was reflected in the numerical models by adjusting the radius of the outer fluid region, $r_o$, which is also half of the allowable distance between two fibres. The radius used is dependent on the ε value and external radius of the hollow fibre, $r_e$. The equation used to determine $r_o$ is as such:

$$\varepsilon = 1 - \left(\frac{\pi(r_e{}^2)}{2\sqrt{3}(r_o{}^2)}\right) \qquad (1)$$

**2.2. Meshing approach**

The mesh was designed using the approach of nodal distribution. For every 0.1 metres of the fibre, 1001 nodes (1000 divisions) were distributed evenly along its length. As for the nodal distribution along the radial direction, 21 and 16 nodes were evenly distributed along membrane and permeate region respectively. For the feed region, the number of nodes depends on the length $r_o$.0.02mm distance between 2 nodes was used as a guideline for radial node distribution across the feed region. This resulted in the model with ε value of 0.8 having 31 nodes distributed evenly while the model withε value of 0.4 having 26 nodes ($r_o$ reduces in length as packing density increases, denoting lesser space between 2 fibres). A mapped mesh function is included to ensure uniform mesh across the entire model. The resulting mesh (Figure 3) takes the form of uniform rectangular element. These elements are fully orthogonal (orthogonal quality = 1) and have skewness values below $10^{-8}$.

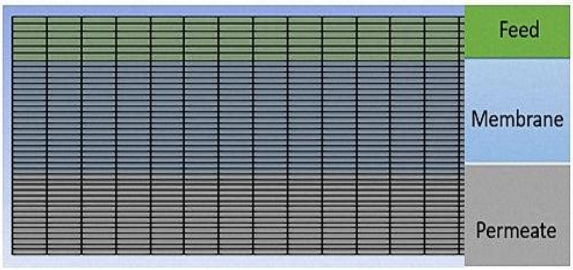


**Fig. 3.** Mesh layout of geometry used.

**2.3. Simulation set-up**

Settings similar to those from past literature (Gunther et al., 2010; Zhuang et al., 2015; Lim et al., 2016) were used. This is to facilitate replication of results for validation purposes. The simulation was ran using the laminar model. Filtration process was simulated with pure water flowing at 30$^{o}$C. As such, density and viscosity are set to 995.6 kg/m$^3$ and 7.972 X $10^{-4}$ Pa.s respectively. Inlet for feed water was set as pressure-inlet with a gauge pressure of 1 bar. Likewise, the outlet for permeate was set as pressure-outlet with a gauge pressure of 0 bar. This is to simulate filtered water flowing out of the hollow fibre at atmospheric pressure. Operating pressure was set as 1.01325 bar, the atmospheric pressure as ground level. The hollow fibre use in our studies has an inner and outer diameter of 0.625mm and 1.5mm respectively. The membrane region was modelled as a porous zone, with viscous resistance set to 5.55 X $10^{14}$, corresponding to a membrane flux of 1500LMH. The porosity of the membrane was kept at 0.7 throughout the study. The SIMPLE discretization scheme was used to determine the pressure and velocity field. For the interpolation of pressure field, the "PRESTO" was selected for its suitability for flows involving steep pressure gradient. The velocity field was interpolated using second order upwind scheme.

**3. Validation against past literature**

Validation of the setting was done by recreating the results of one of the cases documented in the research paper (Zheng et al., 2015). The case taken from the original literature was of a single-end hollow fibre with packing density, ϕ = 0.8. All settings used followed closely to that from their paper. The aim of this validation to know if the turbulence model and solver settings used give consistent result.

Figure 4 and Figure 5 below shows the comparison of our CFD results compared to CFD results from the original literature (Zheng et al., 2015). Comparisons were made to the pressure distribution along the fibre length in the feed and permeate region. Based on comparison of feed pressure distribution (Figure 4), largest difference

in pressure at any point of length was found at the outlet end of the fibre, which had a percentage difference of 4.3%. For the comparison of permeate pressure distribution (Figure 5), largest difference in pressure at any point of length was found at the sealed end of the fibre, with a percentage difference of 2.8%, which gives enough indication that the numerical prediction achieved were consistent with existing data (Zheng et al., 2015). As such, concluding the numerical approach (in terms of the mesh, turbulence model and numerical solver) is validated.

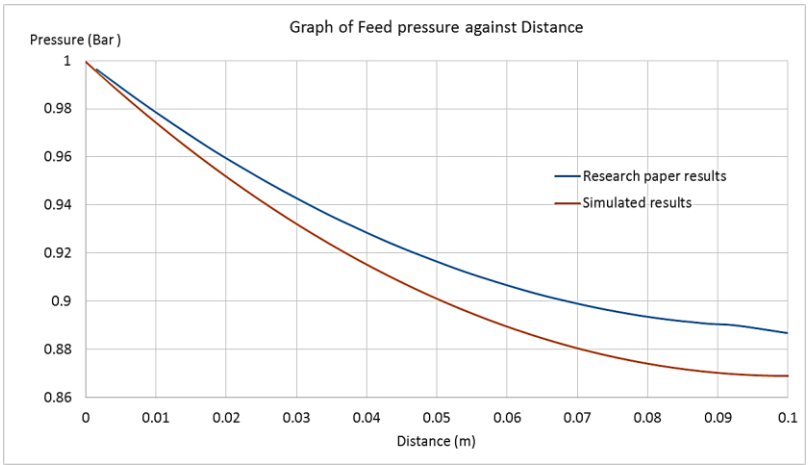


**Fig. 4.** Graph of permeate pressure against distance, for case of epsilon = 0.2 compared against results from original literature.

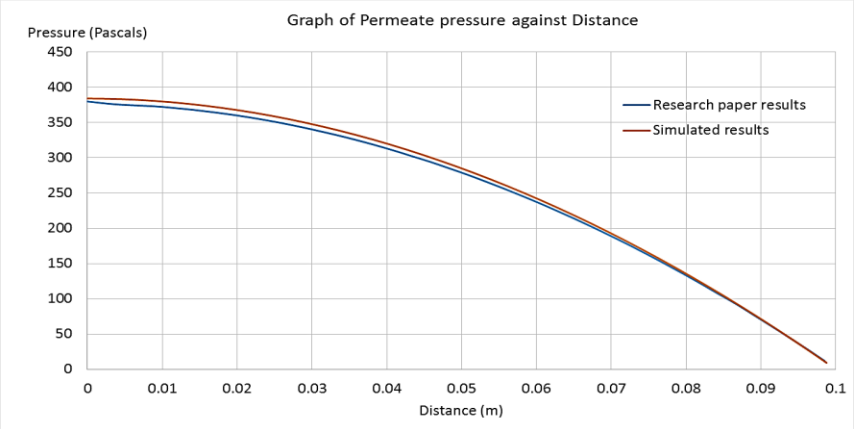


**Fig. 5.** Graph of permeate pressure against distance, for case of epsilon = 0.2 compared against results from original literature.

## 4. Case studies

### 4.1. The effect of packing density on TMP distribution and output volumetric flowrate

#### 4.1.1. Case set-up

Several cases of double-end hollow fibre were simulated based on ε values of 0.2 to 0.8 at an increment of 0.1. Each of the7 different cases was set using fibres with length of 1 metre and 2 metres respectively. This make a total of 14 cases being simulated for this part of the study, each with different set of ε value and fibre length imposed. As stated before in Section 2a, the packing density is reflected in the model by changing the allowable space between 2 fibres. In terms of the 2 dimensional geometry used, this translates to the height of the feed region. Table 1 shows the geometry values used for each ε values used. Height of the membrane wall and permeate region were kept constant at 0.4375mm and 0.3125mm respectively.

**Table 1**
Geometry values of respective ε value.

| Epsilon values, ε | $r_o$ (m) | $r_o$ (mm) | Height of feed region (mm) |
|---|---|---|---|
| 0.2 | 0.000799 | 0.799 | 0.049 |
| 0.3 | 0.000853 | 0.853 | 0.103 |
| 0.4 | 0.000922 | 0.922 | 0.172 |
| 0.5 | 0.001010 | 1.010 | 0.260 |
| 0.6 | 0.001129 | 1.129 | 0.380 |
| 0.7 | 0.001304 | 1.304 | 0.554 |
| 0.8 | 0.001597 | 1.597 | 0.847 |

#### 4.1.2. Results

Figure 6 shows the transmembrane pressure (TMP) distribution along fibre length of 1 metre long double-end hollow fibres with ε values ranging from 0.2 to 0.8. The TMP distribution graph was used as indicator for performance, due to its proportional relationship to membrane flux as stated in Darcy's Law (Darcy, 1856).

$$J = \frac{TMP}{\mu\, R_m} \qquad (2)$$

Where J is membrane flux, μ is viscosity of water and $R_m$ is hydraulic resistance of the membrane wall.

With reference to equation 2, a larger TMP would indicate a higher flux, leading to higher output performance. Based on Figure 6, as the ε value increases, the TMP distribution along fibre length improves. This effect is most significant at the middle section of the fibre, where TMP is lowest at this point. The increment of TMP value at this point is also observed to be the largest when going from ε value of 0.2 to 0.3. Subsequent increase in ε value gave decreasing rate of improvement in TMP value. As the ε value goes beyond 0.6, no significant change in TMP distribution can be observed. This is shown in Figure 7, where the TMP distribution of hollow fibres with ε values of 0.6, 0.7 and 0.8 are all the same.

Cases simulated using the 2 metre long double-end hollow fibre showed similar trend in TMP distribution. However, due to increase in fibre length, lower TMP values were noted at the middle section of the fibre, for all cases of ε value. This finding is consistent with pass literature by T. Carroll and N.A. Booker (2000), which states that fibre of shorter length have better flux compared to fibre of longer length. The result obtain on flux distribution could also be justified as it displays the same curve trend from existing research paper (Li et al., 2014), where numerical simulation were used to predict and obtain flux distributions of double-end hollow fibre module configuration.

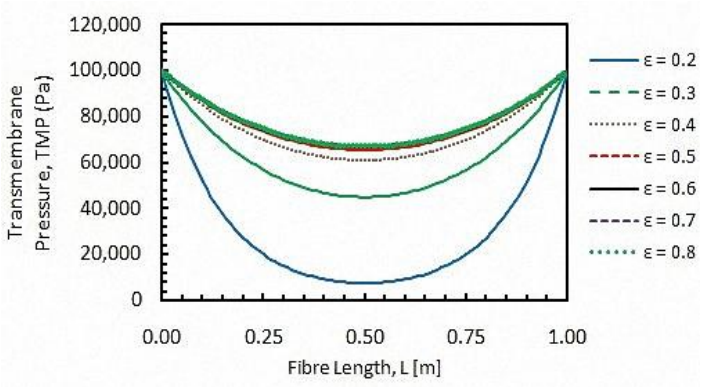


**Fig. 6.** Transmembrane Pressure distribution along length of fibre of 1 metre long double-end fibre, for all epsilon values studied.

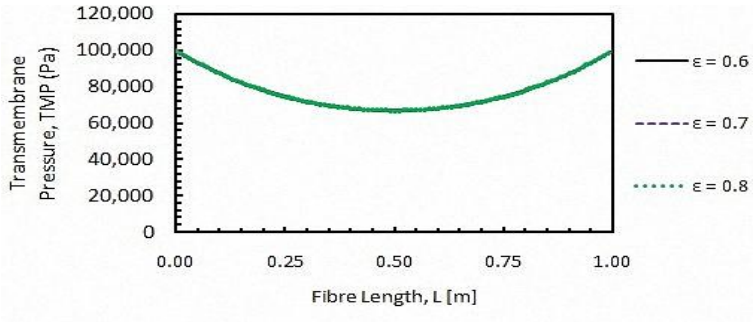


**Fig. 7.** Transmembrane Pressure distribution along length of fibre of 1 metre long double-end fibre, for epsilon values of 0.6, 0.7 and 0.8

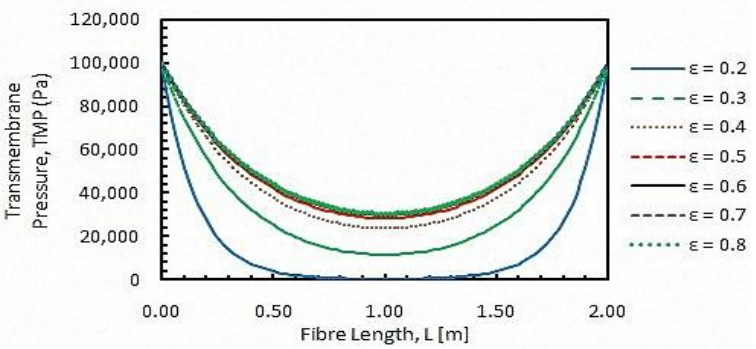


**Fig. 8.** Transmembrane Pressure distribution along length of fibre of 2 metres long double-end fibre, for all epsilon values studied.

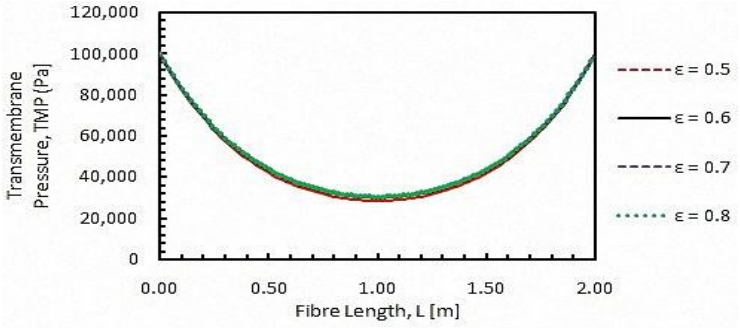


**Fig. 9.** Transmembrane Pressure distribution along length of fibre of 2 metres long double-end fibre, for epsilon values of 0.6, 0.7 and 0.8

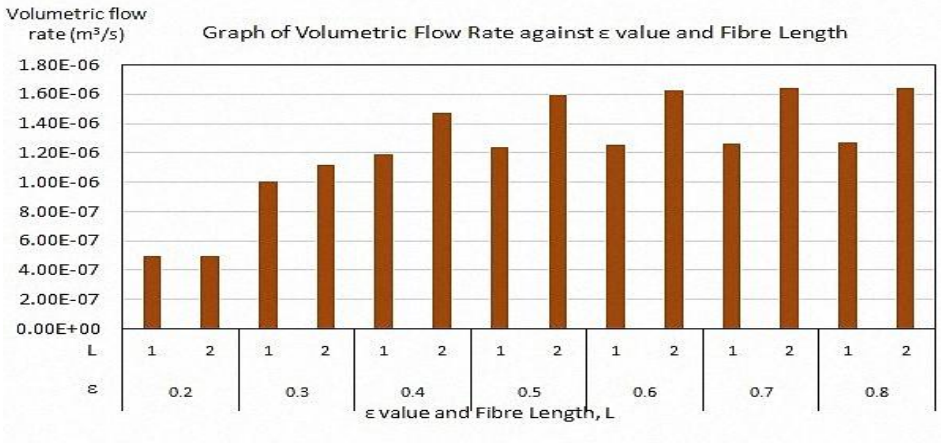


**Fig. 10.** Chart of Volumetric flow rate against ε value and Fibre Length.

In addition to the TMP distributions, the output volumetric flowrate for all 14 cases were also tabulated into a bar chart, shown in Figure 10. When comparing the results of 1m fibre against 2 m fibre of each value of ε, the difference in volumetric flowrate increase as ε value increases from 0.2 to 0.6. This could indicate that increase in output due to increase in length is dependent on the packing density of the module. It is also observed that cases with ε values of 0.6, 0.7 and 0.8 have similar trends in output volumetric flowrate. This is consistent with the TMP distribution plots from Figure 6 and 8, which indicates that increasing ε value beyond 0.6 does not improve the performance of hollow fibres in double-end configuration.

### 4.2. Location of inlet and its effects on feed pressure distribution and overall performance

#### 4.2.1. Case set-up

Three cases of 2 metres long hollow fibre with double-end configuration were set with different inlet location. 2 metres long fibres were used for this study as they have larger drop in pressure distribution along fibre length. The first case had the default configuration, with inlet located at each end of the fibre. The second case had 2 inlets 50mm wide, located along the top boundary of the feed region. The inlets were located 950mm apart of each other. The last case 4 inlets 50mm wide, located along the top boundary of the feed region. The inlets were located 450 mm apart of each other. The layout of these 3 cases were illustrated in Figure 11. All inlet were set at to pressure inlet at 1 bar to ensure consistency in pressure conditions. In addition, all cases were set with packing density of ε = 0.6.

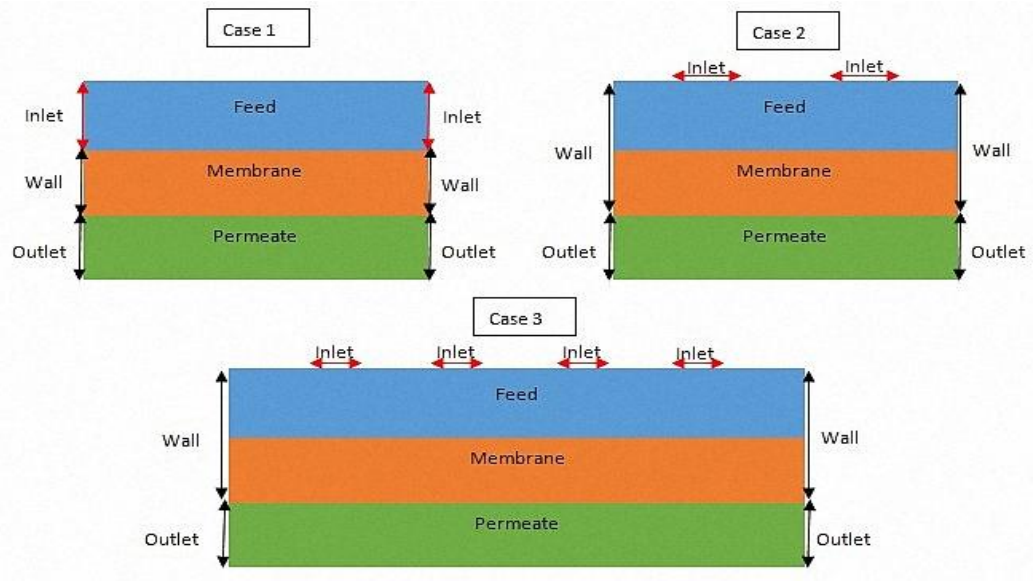


**Fig. 11.** Illustration of location of inlet (red arrow) for each of the 3 case set-up.

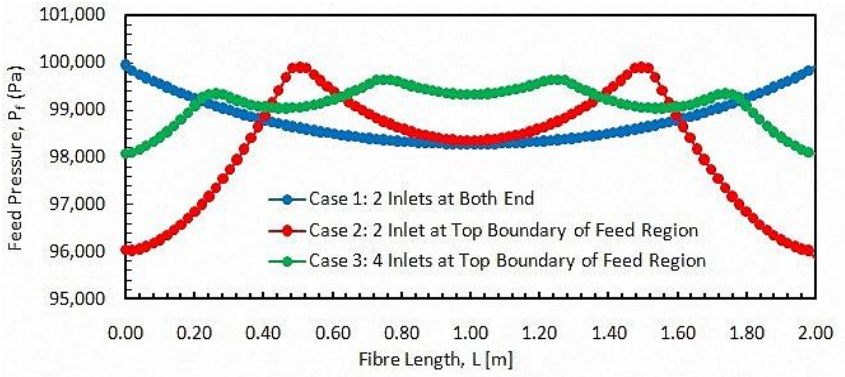


**Fig. 12.** Feed pressure distribution along fibre length of all 3 cases affected by different inlet boundary conditions.

#### 4.2.2. Results

Based on Figure 12, feed pressure distribution of case 2, when compared that of case 1, had higher feed pressure distribution along the centre of the fibre. This is due to the change of inlet location from both ends to locations nearer to the centre of the fibre length. However in this comparison, a dip in feed pressure can be noticed nearing the fibre ends. This issue was improved when the number of inlets were increased to 4. This made the feed pressure distribution more uniform in case 3, as compares the other 2 cases. From Section 4a, it is concluded that feed pressure distribution heavily affected by packing density. This led to the conclusion that for hollow fibre modules that are more densely packed with larger drop infeed pressure drop, the configuration from case 3 may be more ideal.

## 5. Conclusion

Double-end hollow fibres of different packing density, length and location of inlets were studied using numerical methods. The aim of this study was to determine the effects of packing density and location of inlet have on the pressure distribution and output flowrate of double-end hollow fibres. From the above studies, the following conclusions were made:

1. The transmembrane pressure and output volumetric flowrate of double-end hollow fibres improves as ε increases. Such improvement is significant when ε increases from 0.2 to 0.6, where large increase in output flowrate can be observed. Increasing ε beyond 0.6 is not beneficial, as no changes in feed pressure distribution and output flowrate can be observed.

2. The effects of packing density on double-end hollow fibre is consistent to that of single-end hollow fibre. Showing improvements in performance when fibres are less densely packed.

3. Configuration of inlet conditions, in particular its location, greatly affects the distribution of feed pressure along fibre length. Having increased number of inlet along the fibre length improves the uniformity of feed pressure distribution.

## Acknowledgements

The authors acknowledge the Enterprise and Innovation Hub (E.I. Hub), Singapore Institute of Technology (SIT) for their support and funding (E.I. Hub Ignition Grant) for this research project. The authors would also like to acknowledge Ng Kai Sian, final year student in SIT for his contributions to their research project.

## References

Carroll, T., Booker, N.A., 2000. Axial features in the fouling of hollow fibre membranes. J. Membr. Sci., 168, 203-212.

Darcy, H., 1856. Les Fontaines Publiques de la Ville de Dijon, Dalmont, Paris.

Doshi, M.R., Gill, W.N., Kabadi, V.N., 1997. Optimal design of hollow fiber modules. AlChE J., 23, 765-767.

Gunther, J., Schmitz, P., Albasi, C., Lafforgue, C., 2010. A numerical approach to study the impact of packing density on fluid flow distribution in hollow fibre module. J. Membr. Sci., 348, 277-286.

Happel, J., 1959. Viscous flow relative to arrays of cylinders. AlChE J., 5, 174-177.

Li, X.H., Li, J.X., Wang, J., Wang, H., He, B.Q., Zhang, H.W., Guo, W.S., Ngo, H.H., 2014. Experimental investigation of local flux distribution and fouling behaviour indouble-endand dead-end submerged hollow fiber membrane modules. J. Membr. Sci., 453, 18-26.

Lim, K.B., An, H., Wang, P.C., 2016. Evaluation of optimum packing density for cross-flow hollow fibre membranes of different lengths using CFD. IRC conference on science, engineering, and technology 2016.

Soltanieh, M., Gill, W.N., 1983. A note on the effect of fibre length on the productivity of hollow fibre modules. Chem. Eng. Commun., 22, 109.

Zhuang, L., Guo, H., Wang, P., Dai, G., 2015. Study on the flux distribution in a dead-end outside-in hollow fibre membrane module. J. Membr. Sci., 495, 372-383.

**How to cite this article:** Lim, K.B., Wang, P.C., An, H., 2016. Numerical investigation on packing density and inlet configurations of hollow fibres and their effects on flow pattern within ultrafiltration modules. Scientific Journal of Environmental Sciences, 5(11), 269-278.